Cluster-variation calculation for random-field systems: Application to hydrogen in niobium alloys

I. R. MacGillivray, C. E. Soteros, and C. K. Hall
Department of Chemical Engineering, North Carolina State University, Raleigh, North Carolina 27695-7905
(Received 22 September 1986)

The cluster-variation method is applied to random-field lattice systems and specifically used to model the disorder-disorder phase transition of hydrogen in niobium-molybdenum and niobium-vanadium alloys. A small concentration of molybdenum or vanadium in the niobium lattice is treated as adding at each hydrogen site a random energy with a known probability distribution. Pairwise interactions between hydrogen atoms are included out to the first fifty shells on the bcc tetrahedral interstitial lattice, allowing for the effect of site blocking for the first three shells. The results show the small and large depression in the critical temperature for $Nb_{1-y}V_yH_x$ and $Nb_{1-y}Mo_yH_x$, respectively, with increasing concentration of V or Mo, as observed in experiments. Comparison is made with Monte Carlo calculations of other workers with use of the same interaction parameters, and the effects of variations in the random-energy distribution are described.

I. INTRODUCTION

In the past, there has been considerable interest in lattice models with random-site energies. Such models are applicable to amorphous materials, hydrogen in metals, and to physical adsorption and chemisorption onto surfaces. The earliest work appears to be that of Hill,[1] who studied the adsorption of molecules on a heterogeneous surface with and without interactions between adsorbed molecules. In recent years[2,3] models of magnetic spin systems have been studied in which the local field conjugate to the spins is random, the so-called random-field Ising model. Morita[4] gave an expression for the free energy of a nonuniform lattice system (or random lattice gas) using cluster techniques and subsequently[5] applied this expression to the random-field Ising model. More recently, Richards[6] has performed calculations for a lattice gas with random-site energies and applied the results to amorphous metal hydrides.

In this paper the cluster variation method[7,8] (CVM) is applied to a random-field lattice system. The technique is general and can, in principle, be used to give solvable expressions for the free energy of any lattice system with random site energies. However, the calculations presented here are specific to the problem of hydrogen in niobium alloys. When a small amount of a substitutional impurity such as molybdenum is absorbed in niobium, the associated hydride can be treated by considering the impurity atoms to add a random energy, with calculable distribution, to each hydrogen site.[9–11] With use of the theory of lattice statics, the H-H interactions and the random-site-energy distribution can be determined. The H-H interaction includes blocking of the first three shells of sites surrounding any occupied site on the bcc tetrahedral interstitial lattice. The thermodynamic properties and phase diagram are calculated using the CVM. This is a considerable improvement over the usual approach in which Monte Carlo methods are used to calculate metal-hydride phase diagrams since it is an analytic technique which is therefore much less expensive and yet is surprisingly accurate. It is especially well suited to the long-range interactions which are characteristic of metal-hydrogen systems. Although the approach is limited to the description of the α-α' transition, the resulting expression for the chemical potential is simple and readily allows for an assessment of the effect of changes in the interaction parameters.

The CVM calculations presented here also apply to H in a pure metal such as niobium. In this case there is no random-site-energy distribution; this is simply expressed by having a random field with "zero" width. Richards[12] has developed an analytic approximation for a lattice gas with long-range interactions, and has applied it to the α-α' (disorder-disorder) transition in Pd-H and Nb-H to yield critical temperatures and concentrations which agree with Monte Carlo calculations to within 10%. In comparison, the CVM used here yields results which agree even more closely with the Monte Carlo calculations. Similarly, a calculation has been made by Boureau[13] based upon theoretical and experimental expressions for the partial entropy and enthalpy of Nb-H, showing that a simple analytical technique can give reasonable results. Both Richard's approximation and the CVM represent improvements over this calculation.

In Secs. II—IV the CVM is briefly reviewed, and the model and theory presented. Calculations are performed for NbH_x, $Nb_{0.95}Mo_{0.05}H_x$, $Nb_{0.85}Mo_{0.15}H_x$, and $Nb_{0.94}V_{0.06}H_x$ and are presented in Sec. V, along with comparisons with the Monte Carlo results. The effects of variations in the parameters of the model are also described. Finally, in Sec. VI the work is concluded with a brief overview of the results obtained.

II. THE MODEL

We consider a lattice model in which the tetrahedral interstitial sites of bcc niobium are either singly occupied or unoccupied by H atoms (see Fig. 1). Molybdenum atoms (or other impurities) are dissolved substitutionally at random in the niobium lattice. The H atoms interact pairwise with each other and with neighboring Mo atoms with strengths which have been calculated previously as described by Shirley *et al.*[10] In addition to phonon terms, the system Hamiltonian contains the following term which depends on hydrogen concentration:

$$H=\sum_{a,b} V_{ab}\tau_a\tau_b+\tfrac{1}{2}\sum_{a,c} V_{ac}\tau_a\sigma_c \ , \tag{1}$$

where V_{ab} (V_{ac}) is the total interaction energy, respectively, between an H at interstitial site a and an H (Mo) at interstitial (lattice) site b (c). The occupation variable τ_a equals 1 or 0 depending on whether interstitial site a is occupied or unoccupied by an H. Similarly σ_c equals 0 if lattice site c is occupied by an Nb atom and equals 1 if it is occupied by an Mo atom. If this Hamiltonian is rearranged to give

$$H=\sum_{a,b} V_{ab}\tau_a\tau_b+\sum_a \epsilon_a\tau_a \ , \tag{2}$$

where

$$\epsilon_a=\sum_c V_{ac}\sigma_c \ , \tag{3}$$

then the system may be interpreted as a lattice gas with a random energy ϵ_a (or random field) at each site a. The probability that any particular site has a potential energy ϵ is $\rho(\epsilon)d\epsilon$ where $\rho(\epsilon)$ is the random-site-energy probability distribution which is calculable from Eq. (3) as described by Shirley *et al.*[10] If the concentration of the Mo were zero then $\rho(\epsilon)=\delta(\epsilon-\epsilon_0)$, where ϵ_0 is some arbitrary energy. The addition of Mo yields a spread in this energy distribution, characterized by a new $\rho(\epsilon)$. In reality the distribution would not be truly random because of the correlation of energies between nearby sites, but this effect is being neglected. The H-H interactions also change upon addition of the Mo.

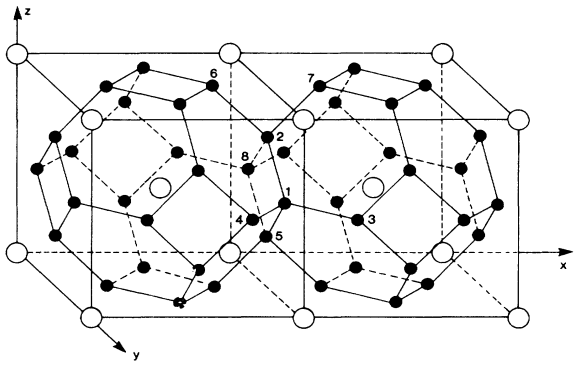

FIG. 1. The bcc host-metal lattice (large open circles) and the tetrahedral interstitial lattice (small solid circles). A typical 5-site tetrahedral cluster is indicated by the sites numbered 1—5. Site 1 is the center of this cluster (cluster 1) and sites 2—5 are at nearest-neighbor separations from site 1. Sites 1, 2, 6, 7, and 8 represent another 5-site cluster centered on site 2 (cluster 2) which overlaps cluster 1 in the 2-site cluster of sites 1 and 2. Similarly, cluster 8 overlaps cluster 1 at the second-neighbor 2-site cluster composed of sites 2 and 5. Clusters 1 and 6, however, only overlap at the 1-site cluster which is site 2.

In order to deal with a continuous energy distribution in the context of the CVM, $\rho(\epsilon)$ will be approximated by a discrete spectrum of Γ energy levels ϵ_α, each characterized by the probability a_α. The distribution is normalized such that

$$\int_{-\infty}^{\infty}\rho(\epsilon)d\epsilon=\sum_{\alpha=1}^{\Gamma} a_\alpha=1 \ . \tag{4}$$

Since the distribution $\rho(\epsilon)$ is typically multipeaked, its approximation by a discrete distribution is justified.

The CVM gives an approximation for the configurational entropy of a system in terms of the concentration of cluster configurations on the lattice. A cluster is a set of lattice sites forming an arbitrary geometrical figure, and a configuration is a particular arrangement of particles on a cluster. Following the notation of Sanchez and de Fontaine,[7] the entropy in the CVM is

$$S=Nk_B\sum_{(r,t)}\gamma(r,t)\sum_l \alpha_l(r,t)x_l(r,t)\ln x_l(r,t) \ , \tag{5}$$

where N is the total number of lattice points or sites and k_B is Boltzmann's constant. The index t in (r,t) labels a specific type of r-site cluster. In the systems considered here each interstitial site can be either occupied or unoccupied by a hydrogen atom. Therefore there are generally 2^r arrangements or configurations of an (r,t) cluster, although some will be equivalent. The variable $x_l(r,t)$ is the concentration of the lth configuration of the (r,t) cluster, and $\alpha_l(r,t)$ is a degeneracy factor which takes into account the configurations which are equivalent. If the full 2^r configurations are enumerated separately then $\alpha_l(r,t)=1$. A particular configuration l is specified by the r numbers $\{i,j,\ldots,k\}$ where each number takes the value 1 if the site is occupied and -1 otherwise. The largest clusters to be considered must be chosen in advance in order to calculate S using Eq. (5). These clusters are called the basic clusters and contain $\bar{n}$ points. There can be many independent basic clusters with different values of $\bar{n}$. The coefficients $\gamma(r,t)$ are given by

$$\gamma(\bar{n},t)=-N(\bar{n},t)/N \tag{6}$$

for the basic clusters and by

$$\gamma(r,t)=-N(r,t)/N-\sum_{q=r+1}^{\bar{n}}\sum_s M(r,t;q,s)\gamma(q,s) \ , \qquad 1\le r<\bar{n} \tag{7}$$

for all other clusters, where $N(r,t)$ is the total number of (r,t) clusters in the system and $M(r,t;q,s)$ is the number of (r,t) clusters contained in a (q,s) cluster. For any (r',t') cluster which is completely contained in an $(\bar{n},t)$ basic cluster and is not shared by any other basic clusters,

$$N(r',t')=M(r',t';\bar{n},t)N(\bar{n},t) .$$

Using this relationship in Eqs. (6) and (7) results in $\gamma(r',t')=0$. Hence the only nonzero contributions to the entropy come from clusters formed from the intersection of two basic clusters, or from the intersections of other clusters for which $\gamma(r,t)$ is nonzero. $N(r,t)$ and $M(r,t;q,s)$ are calculated straightforwardly as described by Sanchez and de Fontaine.

Once the largest clusters are chosen the entropy can be expressed in terms of the cluster concentrations using Eq. (5). By minimizing the free energy (or the grand potential, as discussed in Sec. IV) the equilibrium cluster concentrations can be determined, enabling the chemical potential and phase diagram of the system to be calculated. Although the tetrahedral interstitial lattice is not a Bravais lattice and possesses six different sites from the viewpoint of translational symmetry, each lattice site is equivalent from the point of cluster algebra since each site has the same number of nth neighbors at the same distances, arranged in the same general way. It is therefore not necessary to distinguish between the different site types when applying the CVM.

Boureau[13] has shown that experimental measurements of the partial molar entropy support a H-H interaction that is infinitely repulsive out to second neighbors on the tetrahedral lattice. But to obtain reasonable phase diagrams previous workers[9–11,14–16] have used a blocking model that extends to third neighbors. Therefore, in order to compare the model used here with previous Monte Carlo calculations and to achieve a phase diagram which compares well with experiment the blocking will be regarded as extending to third neighbors. While this can be allowed for by setting the appropriate interaction energies to infinity it is better to account for this directly when choosing the basic clusters for the CVM expansion. It can be also be noted that these near-neighbor repulsions should partially negate the effect of correlations between the random energies of nearby hydrogen atoms since in this case the hydrogen atoms are never close together.

In this model the basic clusters chosen form two distinct sets. The first set contains the five-site (tetrahedral) clusters which consist of a site and its four nearest neighbors (see, for example, cluster 1 in Fig. 1). Each site will have an energy which is one of the Γ values of ϵ_α, so a particular cluster can be specified by the indices $(5,\alpha,\beta,\gamma,\delta,\zeta)$ if site 1 of the cluster (the center) has energy ϵ_α, site 2 has energy ϵ_β, and so on. For simplicity in the calculations, symmetry will not be used to reduce the number of distinct clusters to less than 5^Γ [even though, for example, $(5,\alpha,\beta,\gamma,\delta,\zeta)$ and $(5,\alpha,\beta,\gamma,\zeta,\delta)$ are equivalent] and the indices $\alpha-\zeta$ are considered to be ordered. These 5-site clusters are used to account for the exclusion out to third neighbors.

The second set of basic clusters is chosen to allow for the long-range interactions that are needed to more accurately take account of the phase change. It consists of all nth-neighbor pairs for $n\geq 4$ out to some finite limit $n=L$. In a similar manner to the 5-site clusters, the 2-site basic clusters may be written as $(2,\alpha,\beta,n)$ where $n\geq 4$. These clusters are independent of the 5-site clusters and, again, a $(2,\alpha,\beta,n)$ cluster is considered distinct from a $(2,\beta,\alpha,n)$ cluster if $\alpha\neq\beta$.

III. CONFIGURATIONAL ENTROPY

In the bcc interstitial lattice two 5-site tetrahedral clusters can overlap in only three ways, as shown in Fig. 1. If the centers of the adjacent clusters are nearest neighbors then the region of overlap is simply the nearest-neighbor pair formed by these centers. If the separation of the centers is a second-neighbor distance then the overlapping region is another second-neighbor pair. Last, if the centers are at a third-neighbor separation then only a single site is common. Similarly, a particular 2-site $n>3$ cluster can overlap another distinct 2-site or 5-site cluster only at one site. Hence, the only subclusters on the lattice for which $\gamma(r,t)$ in Eq. (5) is nonzero are of the type $(2,\alpha,\beta,n=1)$, $(2,\alpha,\beta,n=2)$, or $(1,\alpha)$.

As the total number of sites is N, and the site energies are assumed to be randomly distributed over the sites, the number of 1-site clusters of a particular type is

$$N(1,\alpha)=a_\alpha N . \tag{8}$$

There are a total of N 5-site clusters as every site is the center of such a cluster. Hence,

$$N(5,\alpha,\beta,\gamma,\delta,\zeta)=a_\alpha a_\beta a_\gamma a_\delta a_\zeta N \tag{9}$$

since the probability a_α that any site has energy ϵ_α is independent of the energy of any other site.

The number of nth neighbors of a particular site on the interstitial lattice will be denoted by z_n. In an infinite lattice there are a total of $Nz_n/2$ nth-neighbor pairs. The number of $(2,\alpha,\beta,n)$ clusters is therefore

$$N(2,\alpha,\beta,n)=a_\alpha a_\beta z_n N/2 . \tag{10}$$

The above results are summarized in Table I.

Values of $\gamma(r,t)$ are obtained using Eqs. (6) and (7). The number of (r,t) clusters contained in a (q,s) cluster, $M(r,t;q,s)$ is obtained from the geometry of the particular clusters. For each basic cluster $\gamma(\bar{n},t)$ is obtained using Eq. (6) and given in Table I. Values of $\gamma(r,t)$ for the subclusters are obtained using Eq. (7) for successively lower values of r, and are also shown in the table.

For example,

$$M(2,\alpha,\beta,1;5,\alpha',\beta',\gamma',\delta',\zeta')=\delta_{\alpha\alpha'}(\delta_{\beta\beta'}+\delta_{\beta\gamma'}+\delta_{\beta\delta'}+\delta_{\beta\zeta'}) , \tag{11}$$

TABLE I. The number $N(r,t)$ of (r,t) clusters on the lattice and nonzero values of the parameter $\gamma(r,t)$ that appears in Eq. (5).

(r,t) cluster	$N(r,t)/N$	$\gamma(r,t)$
$(5,\alpha,\beta,\gamma,\delta,\zeta)$	$a_\alpha a_\beta a_\gamma a_\delta a_\zeta$	$-a_\alpha a_\beta a_\gamma a_\delta a_\zeta$
$(2,\alpha,\beta,n)$, $4\leq n\leq L$,	$a_\alpha a_\beta z_n/2$	$-a_\alpha a_\beta z_n/2$
$(2,\alpha,\beta,1)$	$2a_\alpha a_\beta$	$2a_\alpha a_\beta$
$(2,\alpha,\beta,2)$	$a_\alpha a_\beta$	$a_\alpha a_\beta$
$(1,\alpha)$	a_α	$a_\alpha\left[-2+\sum_{n=4}^{L} z_n\right]$

since the function is nonzero only if the central site of the 5-site cluster is of energy ϵ_α and one (or more) of the other four sites is of energy ϵ_β. Then from Eq. (7),

$$\gamma(2,\alpha,\beta,1)=-\frac{N(2,\alpha,\beta,1)}{N}+\sum_{\alpha'\beta'\gamma'\delta'\zeta'} M(2,\alpha,\beta,1;5,\alpha',\beta',\gamma',\delta',\zeta')a_{\alpha'}a_{\beta'}a_{\gamma'}a_{\delta'}a_{\zeta'}=2a_\alpha a_\beta \ . \tag{12}$$

In this expression the normalization condition (7) has been used and all sums are performed over the Γ values of the energy index for each $\alpha,\beta,\ldots$. [Note that the right-hand side of Eq. (11) depends on the ordering chosen for the sites of the clusters with respect to the notation; however, the result of Eq. (12) is independent of the choice.] Coefficients $\gamma(2,\alpha,\beta,2)$ and $\gamma(1,\alpha)$ are obtained in a similar manner.

Note all the cluster concentrations $x_l(r,t)$ in Eq. (5) are independent. If x_α is the probability that a site of energy ϵ_α is occupied then the probability that it is not occupied is $1-x_\alpha$, so that two 1-site configurations have concentrations

$$\begin{aligned} &x_1(1,\alpha)=x_\alpha \ , \\ &x_{-1}(1,\alpha)=1-x_\alpha \ . \end{aligned} \tag{13}$$

Each of the basic 2-site clusters has the four configurations $\{1,1\}$, $\{1,-1\}$, $\{-1,1\}$, and $\{-1,-1\}$. Straightforward probability arguments show that, for example,

$$x_1(1,\alpha)=x_{1,1}(2,\alpha,\beta,n)+x_{1,-1}(2,\alpha,\beta,n) \ , \tag{14}$$

and if $x_{1,1}(2,\alpha,\beta,n)$ is written in the more compact form $x_{\alpha\beta;n}$ then the 2-site concentrations can be given in terms of the x_α and $x_{\alpha\beta;n}$:

$$\begin{aligned} &x_{1,1}(2,\alpha,\beta,n)=x_{\alpha\beta;n}, \quad 4\le n\le L \\ &x_{1,-1}(2,\alpha,\beta,n)=x_\alpha-x_{\alpha\beta;n}, \quad 4\le n\le L \\ &x_{-1,1}(2,\alpha,\beta,n)=x_\beta-x_{\alpha\beta;n}, \quad 4\le n\le L \\ &x_{-1,-1}(2,\alpha,\beta,n)=1-x_\alpha-x_\beta+x_{\alpha\beta;n}, \quad 4\le n\le L \ . \end{aligned} \tag{15}$$

To reduce the 5-site and 2-site ($n=1,2$) cluster concentrations, as for Eqs. (13) and (15), the correlation functions of Sanchez and de Fontaine are introduced. Let

$$\Gamma_i(p)=\tfrac{1}{2}[1+i\sigma(p)] \ , \tag{16}$$

$$\sigma(p)=\begin{cases} +1 \ \text{(site } p \text{ occupied)} \ , \\ -1 \ \text{(site } p \text{ unoccupied)} \ , \end{cases}$$

where i takes the value 1 if p is occupied and -1 if p is unoccupied. Then $\Gamma_i(p)$ is unity if p is occupied ($i=1$) and zero otherwise ($i=-1$). The cluster concentrations become

$$\begin{aligned} x_{i,j,\ldots,k}(r,t)&=\frac{1}{N(r,t)}\sum_{\{p_1,\ldots,p_r\}_t}\Gamma_i(p_1)\Gamma_j(p_2)\cdots\Gamma_k(p_r) \\ &=\frac{1}{2^r}\left[1+\sum_{(r',t')} v_{i,j,\ldots,k}(r,t;r',t')\xi(r',t')\right] \ , \end{aligned} \tag{17}$$

where

$$\xi(r',t')=\frac{1}{N(r',t')}\sum_{\{p_1,\ldots,p_{r'}\}_{t'}}\sigma(p_1)\sigma(p_2)\cdots\sigma(p_{r'}) \tag{18}$$

is the r'-body correlation function and $v_{i,j,\ldots,k}(r,t;r',t')$ is, in general, a sum of r'-order products involving the indices $i,j,\ldots,k$. The symmetry of the cluster determines the form of $v_{i,j,\ldots,k}(r,t;r',t')$, as described by Sanchez and de Fontaine, and the sum in Eq. (17) is taken over all lattice points $p_1,\ldots,p_r$ consistent with the (r,t) cluster.

For the 1- and 2-site clusters, Eqs. (16)—(18) give

$$x_i(1,\alpha)=\tfrac{1}{2}[1+i\xi(1,\alpha)] \ , \tag{19}$$

$$x_{i,j}(2,\alpha,\beta,n)=\tfrac{1}{4}[1+i\xi(1,\alpha)+j\xi(1,\beta)+ij\xi(2,\alpha,\beta,n)] \quad \text{for all } n \ . \tag{20}$$

But $x_{1,1}(2,\alpha,\beta,n)=0$ for $n\le 3$ since two sites with first-, second-, or third-neighbor separations cannot both be occupied. Hence, from Eqs. (13), (19), and (20),

$$\xi(2,\alpha,\beta,n)=1-2x_\alpha-2x_\beta \tag{21}$$

and

$$\begin{aligned} &x_{1,1}(2,\alpha,\beta,n)=0, \quad n\le 3 \\ &x_{1,-1}(2,\alpha,\beta,n)=x_\alpha, \quad n\le 3 \\ &x_{-1,1}(2,\alpha,\beta,n)=x_\beta, \quad n\le 3 \\ &x_{-1,-1}(2,\alpha,\beta,n)=1-x_\alpha-x_\beta, \quad n\le 3 \ . \end{aligned} \tag{22}$$

This result can also be obtained by setting $x_{\alpha\beta;n}=0$ in Eqs. (15).

In order to determine the 5-site-cluster concentrations it is convenient to first consider all possible 3- and 4-site clusters, even though they are not directly needed in the equation for the entropy. There are two types of 3-site α,β,γ clusters that can be constructed from the sites of the 5-site cluster—one contains the central site and the other does not. In either case an $x_{i,j,k}(3,\alpha,\beta,\gamma)$ can be obtained in terms of the correlation functions and $x_{1,1,1}(3,\alpha,\beta,\gamma)$ then set to zero as only one site can be occupied. In both cases this gives

$$\xi(3,\alpha,\beta,\gamma)=-1+2x_\alpha+2x_\beta+2x_\gamma \tag{23}$$

so the distinction between the two cases is irrelevant here. Extending this procedure to the 4-site and finally the 5-site clusters gives

$$\begin{aligned} &\xi(4,\alpha,\beta,\gamma,\delta)=1-2x_\alpha-2x_\beta-2x_\gamma-2x_\delta \ , \\ &\xi(5,\alpha,\beta,\gamma,\delta,\zeta)=-1+2x_\alpha+2x_\beta+2x_\gamma+2x_\delta+2x_\zeta \ . \end{aligned} \tag{24}$$

Substituting these results back into Eq. (17) gives

$$x_{i,j,k,l,m}(5,\alpha,\beta,\gamma,\delta,\zeta)=\begin{cases} x_\alpha \text{ if } i=1,\ j=k=l=m=-1\ , \\ x_\beta \text{ if } j=1,\ i=k=l=m=-1\ , \\ \vdots \qquad\qquad \vdots \\ x_\zeta \text{ if } m=1,\ i=j=k=l=-1\ , \\ 1-x_\alpha-x_\beta-x_\gamma-x_\delta-x_\zeta \text{ if } i=j=k=l=m=-1\ , \\ 0 \text{ otherwise}\ . \end{cases} \tag{25}$$

The entropy is obtained by substituting Eqs. (13), (15), (22), and (25), and the expressions for $\gamma(r,t)$ from Table I, into Eq. (5). Simplification then leads to

$$\begin{aligned} S/Nk_B=&-\sum_\alpha a_\alpha x_\alpha \ln x_\alpha-2\sum_\alpha a_\alpha(1-x_\alpha)\ln(1-x_\alpha)+3\sum_{\alpha\beta}a_\alpha a_\beta(1-x_\alpha-x_\beta)\ln(1-x_\alpha-x_\beta) \\ &-\sum_{\alpha\beta\gamma\delta\zeta}a_\alpha a_\beta a_\gamma a_\delta a_\zeta(1-x_\alpha-x_\beta-x_\gamma-x_\delta-x_\zeta)\ln(1-x_\alpha-x_\beta-x_\gamma-x_\delta-x_\zeta) \\ &-\sum_{n=4}^{L}\frac{z_n}{2}\sum_{\alpha\beta}a_\alpha a_\beta[x_{\alpha\beta;n}\ln x_{\alpha\beta;n}+(x_\alpha-x_{\alpha\beta;n})\ln(x_\alpha-x_{\alpha\beta;n})+(x_\beta-x_{\alpha\beta;n})\ln(x_\beta-x_{\alpha\beta;n}) \\ &\qquad+(1-x_\alpha-x_\beta+x_{\alpha\beta;n})\ln(1-x_\alpha-x_\beta+x_{\alpha\beta;n})] \\ &+\sum_{n=4}^{L}z_n\sum_\alpha a_\alpha[x_\alpha\ln x_\alpha+(1-x_\alpha)\ln(1-x_\alpha)]\ , \end{aligned} \tag{26}$$

which is an expression for the entropy of the system of H atoms in terms of the cluster concentrations. When combined with the total energy of the system to give the free energy or grand potential, as in the following section, minimization with respect to the cluster concentrations will give the equilibrium values of all these parameters.

The procedure of this section could, in principle, be used to calculate the entropy for a system with site blocking to any nth-neighbor shell if appropriate basic clusters were chosen. For example, in the system chosen here the basic tetrahedral cluster is convenient because first-, second-, and third-neighbor separations exist in a cluster of this type. This readily allows for an explicit account of site blocking out to third neighbors [Eqs. (16)–(25)]. Although the expression for the entropy would be more complicated, the same basic clusters could be used for first- or second-neighbor blocking. For blocking out to separations larger than third neighbors a larger cluster would give better results.

IV. ENERGY AND GRAND POTENTIAL

For every occupied nth-neighbor pair on the lattice there is an associated interaction energy J_n. There is also a contribution from each occupied site as a result of the imposed random site energies. The total energy of the hydrogen atoms can therefore be written in terms of the cluster concentrations as described below.

Equation (10) gives the number of 2-site clusters of a particular type, and $x_{1,1}(2,\alpha,\beta,n)$ is the fraction that have both sites occupied resulting in an interaction energy J_n. The total interaction energy is therefore obtained by multiplying these three factors together and summing over all cases. Similarly, there are Na_α sites with energy ϵ_α and a fraction x_α of these sites are occupied. Hence the total energy is

$$E=\frac{N}{2}\sum_n z_n J_n\sum_{\alpha\beta}a_\alpha a_\beta x_{\alpha\beta;n}+N\sum_\alpha a_\alpha\epsilon_\alpha x_\alpha\ . \tag{27}$$

The equilibrium configuration of the entire system, specified by particular values of the variables x_α and $x_{\alpha\beta;n}$, is obtained by minimizing the free energy

$$F=E-TS \tag{28}$$

with respect to these variables, subject to the constraint that the total concentration c of H atoms on the lattice is fixed. However, it is more convenient when calculating phase diagrams to consider the grand potential

$$\Omega=F-\mu Nc=E-TS-\mu Nc\ , \tag{29}$$

where μ is the chemical potential of the H atoms. The concentration c can be written in terms of the variables x_α: there are $Na_\alpha x_\alpha$ sites of each energy ϵ_α giving

$$c=\frac{1}{N}\sum_\alpha Na_\alpha x_\alpha=\sum_\alpha a_\alpha x_\alpha\ . \tag{30}$$

Minimizing Ω with respect to the cluster concentration variables ensures that

$$N\mu=\frac{dF}{dc}\ . \tag{31}$$

It also follows that, in equilibrium, two coexisting phases share the same values of Ω and μ.[17]

The grand potential is minimized by setting

$$\frac{\partial\Omega}{\partial x_\alpha}=0\ , \tag{32}$$

$$\frac{\partial\Omega}{\partial x_{\alpha\beta;n}}=0\ . \tag{33}$$

Equation (32) represents Γ equations for Γ variables x_α. Although Eq. (33) represents the number $L\Gamma^2$ of 2-site variables $x_{\alpha\beta;n}$, not all are independent since $x_{\alpha\beta;n}=x_{\beta\alpha;n}$. Using Eqs. (26), (27), (29), and (30), Eqs. (32) and (33), respectively, give

$$\frac{\mu}{k_BT}=\frac{\epsilon_\alpha}{k_BT}+\ln\left[\frac{x_\alpha}{(1-x_\alpha)^2}\right]+6\sum_\beta a_\beta\ln(1-x_\alpha-x_\beta)$$
$$-5\sum_{\beta\gamma\delta\zeta}a_\beta a_\gamma a_\delta a_\zeta(1-x_\alpha-x_\beta-x_\gamma-x_\delta-x_\zeta)\ln(1-x_\alpha-x_\beta-x_\gamma-x_\delta-x_\zeta)$$
$$+\sum_{n=4}^{L}z_n\left[\ln\left[\frac{1-x_\alpha}{x_\alpha}\right]+\sum_\beta a_\beta\ln\left[\frac{x_\alpha-x_{\alpha\beta;n}}{1-x_\alpha-x_\beta+x_{\alpha\beta;n}}\right]\right] \tag{34}$$

and

$$x_{\alpha\beta;n}=\frac{x_\alpha+x_\beta}{2}-\frac{1-\{[1+(x_\alpha-x_\beta)U_n]^2-4x_\alpha(1-x_\beta)U_n\}^{1/2}}{2U_n}, \tag{35}$$

where

$$U_n=1-e^{-J_n/k_BT}. \tag{36}$$

The first term in Eq. (34) is the contribution to μ from the random site energies, while the last term results from the interactions J_n. The remaining terms arise from the clusters chosen to take explicit account of site blocking. For example, the fourfold sum arises from the 5-site cluster configuration with all sites unoccupied.

For a given μ, Eq. (34), which actually represents Γ nonlinear equations in the Γ unknown values of x_α, can be solved numerically for the x_α using the Newton-Raphson method. The concentration c is then obtained using Eq. (30) and Ω is found using Eq. (29). Alternatively, Eq. (30) can be included with Eq. (34), for a fixed value of c, and the equations can then be solved for the $\Gamma+1$ variables x_α and μ, thus giving Ω. A plot of Ω versus μ is then used to determine the values of Ω, μ, and c where phase separation occurs. (Note that it is necessary to add a term corresponding to a long-range elastic interaction in order to obtain the α and α' phases as is discussed further in Sec. V.) For a particular T, the point at which the Ω versus μ curve crosses itself gives the coexistence concentrations on the T versus c phase diagram.

When there are no random site energies, Eqs. (34) and (35) become

$$\frac{\mu}{k_BT}=\ln\left[\frac{(1-2c)^6c}{(1-5c)^5(1-c)^2}\right]-\sum_{n=4}^{L}z_n\ln v_n, \tag{37}$$

$$v_n=\frac{1-y}{2}+\frac{1}{2}[(1-y)^2+4ye^{-J_n/k_BT}]^{1/2}, \tag{38}$$

$$y=\frac{c}{1-c}. \tag{39}$$

This can be compared with the expression derived by Richards[12] for a lattice gas model with many neighbor interactions but no random site energies:

$$\frac{\mu}{k_BT}=\ln\left[\frac{c}{1-c}\right]-\sum_{n=1}^{L}z_n\ln v_n. \tag{40}$$

The second term on the right-hand side of Eq. (37) is the same as Richards's equation (but excludes $n=1,2,3$), and the first term differs because the total exclusion of first- to third-neighbor occupied pairs in our model is taken into account explicitly. If the basic clusters had been chosen to be only the $(2,\alpha,\beta,n)$ clusters [in this case simply $(2,n)$] for all n, with total exclusion taken into account only by setting $J_n=\infty$ (and not by setting the cluster concentrations to zero), then we would have obtained Richards's equation. Richards has also treated the infinite repulsions explicitly and Eq. (37) will be compared with his results in Sec. V.

If there are no interactions beyond the repulsive third-neighbor core equation (37) gives

$$-\frac{\mu}{k_BT}=\frac{1}{Nk_B}\frac{\partial S}{\partial c}=\ln\left[\frac{(1-5c)^5(1-c)^2}{(1-2c)^6c}\right], \tag{41}$$

where the first equality follows from the minimization condition (32). Boureau[18] has derived the following approximation for the partial molar entropy of this system,

$$\frac{1}{Nk_B}\frac{\partial S}{\partial c}=\ln\left[\frac{(1-5c)^4(1-4c)}{(1-2c)^3(1-3c)c}\right], \tag{42}$$

which is a similar functional form and agrees well numerically with Eq. (41), especially for the concentration range of interest ($c\lesssim 0.1$).

The form of Eq. (37) can be compared with the work of Meuffels and Oates,[19] who performed Monte Carlo calculations for a lattice gas with a second-neighbor hard-core and a finite third-neighbor interaction energy. They found that the second-neighbor Boureau expression, combined with Richards's interaction term, gave the best comparison with the simulations. This is completely analogous to our Eq. (37), which combines a "Boureau-like" hard-core and a Richards-type term, both of which arise naturally and more rigorously in this equation through the use of the CVM.

V. PHASE DIAGRAMS

The parameters appearing in Eqs. (34) and (35) are the H-H pairwise interaction energies J_n, the random energies ϵ_α and the weighting factors a_α. In general, the computation of these parameters is a complex task, but various

workers[10,11,14,15] have calculated the random site energy distribution $\rho(\epsilon)$ and the elastic contribution to the J_n for Nb-H, Nb-Mo-H, and Nb-V-H. Use of these data enables a comparison between Eqs. (34) and (35) and the Monte Caro calculations of the phase diagrams also performed by these workers.

In addition to the relatively short-range interactions already discussed the grand potential includes an elastic interaction term associated with the free surfaces of the crystal. Since this term is of macroscopic range it can be treated in mean field theory, resulting in the addition of a term $Nac^2/2$ (where a is a constant) to the free energy and hence to the grand potential. Minimizing the grand potential with respect to the independent cluster concentrations yields the same results as Eqs. (34) and (35) except that μ must be replaced by $\mu - ac$. Equivalently, if μ is the minimized solution to Eqs. (34) and (35), then the solution to the problem when the long-range elastic interaction is included is simply $\mu + ac$. In this work $a/k_B \approx -18\,000$ K when $L \approx 50$.[10,16]

Using the interaction energies calculated by Futran *et al.*,[16] which extend out to $L = 50$ shells, the α-α' coexistence curve in NbH_x, where $x = 6c$, was obtained using Eq. (37) (no random site energies are required). The results are compared in Fig. 2 with the Monte Carlo results of Futran *et al.* for the same system. The critical parameters obtained here are $T_c = 451$ K and $x_c = 0.33$, compared with $T_c = 460$ K and $x_c = 0.29$ for Futran *et al.* the discrepancies being directly attributable to the differences between the Monte Carlo technique and the approximate analytical technique used here. The coexistence curves are in reasonably good agreement, especially considering the simplicity of the technique. At higher hydrogen concentrations the discrepancies are largest, which is in part due to the expression (26) for the entropy being more accurate at low concentrations. Differences also arise because the model used here does not account for the ordering of the H atoms found experimentally for $x \approx 0.6 - 1.0$ (the β phase), whereas the calculations of Futran *et al.* do allow for ordering. (The inclusion of ordering in the CVM model used here is discussed later.) Some experimental results are also included in the figure for reference, but it should be noted that the differences here may be due to many factors, including deficiencies in the models and errors in the interactions J_n and the elastic parameter a. A typical experimental critical point[20] is $T_c = 444$ K, $x_c = 0.31$.

Without explicit account of near-neighbor repulsions Richards[12] obtained $T_c = 520$ K and $x_c = 0.51$ for NbH_x using Eq. (40). When Richards modified his model to explicitly include the infinite repulsions out to third neighbors, T_c was reduced to 421 K and x_c to 0.26.

The thermodynamic factor

$$f_{\text{ther}} = \frac{c}{k_B T}\left[\frac{\partial \mu}{\partial c}\right]_T = \frac{x}{k_B T}\left[\frac{\partial \mu}{\partial x}\right]_T \tag{43}$$

is an experimentally measurable quantity[21] that is readily obtained for NbH_x from Eq. (37). The factor represents averaged information on the effects of the H-H interactions. Figure 3 presents f_{ther} for hydrogen in pure niobium at temperatures near and above the critical temperature for a wide range of concentrations. Comparison of the theory with experiment in Fig. 2, showing a phase envelope which is too wide, indicates that the theoretical

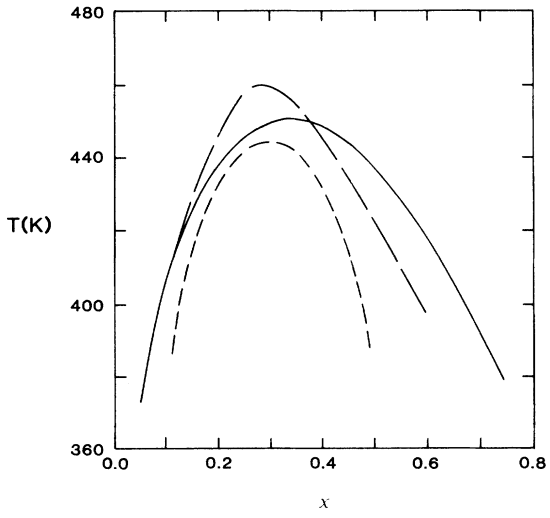

FIG. 2. Phase diagram for the α-α' transition in NbH_x. The solid curve gives the result obtained in this work, the long-dashed curve is the Monte Carlo result of Futran *et al.* (Ref. 16) for the same model, and the short-dashed curve is a typical experimental result (Ref. 20).

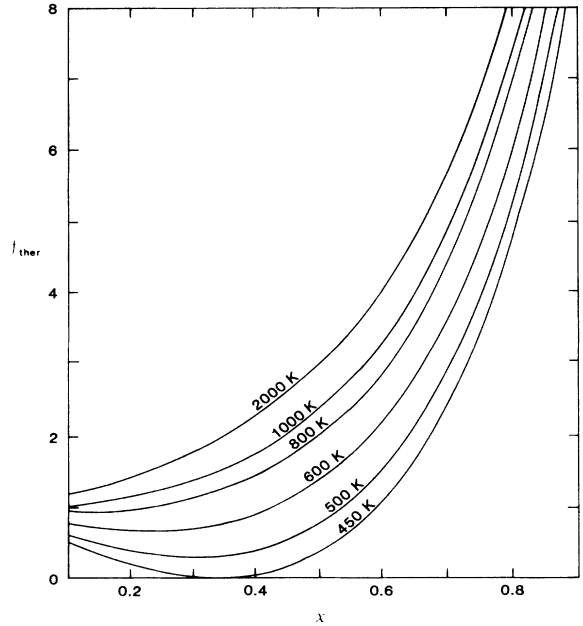

FIG. 3. Thermodynamic factor f_{ther} as a function of concentration for NbH_x as obtained in this work. Curves are given for several temperatures (as indicated) near and above the critical temperature.

f_{ther} obtained here is probably too small at high concentrations. Note that at low concentrations the interaction effects become unimportant and $f_{\text{ther}} \rightarrow 1$ is $c \rightarrow 0$.

To model hydrogen in a niobium alloy using Eqs. (34) and (35) requires that both the interaction energies J_n and random-energy distribution $\rho(\epsilon)$ be known. Shirley *et al.*[10] have determined $\rho(\epsilon)$ and J_n for 5% and 15% molybdenum in niobium. Figure 4 shows the results obtained by using their data in equations (34) and (35). Similarly, Fig. 5 shows the phase diagram obtained using the parameters of Grewell[11] for 6% vanadium in niobium. Table II presents the discrete spectrum of energies, approximating $\rho(\epsilon)$, that was used in each case.

With L, the maximum nth neighbor considered, of order 50, and the number of site energies $\Gamma \approx 5$, Eq. (34) can be solved rapidly to give c for any particular values of μ and T. For $\Gamma \gtrsim 10$, the fourfold energy sum appearing in the equation makes the calculation more time-consuming. However, values much larger than this were found to be unnecessary since increasing Γ led to only small changes in the calculated coexistence curves.

The Monte Carlo calculations of Shirley *et al.* for Nb-Mo-H are also shown in Fig. 4. It can be seen that the addition of as little as 5% Mo to Nb lowers the critical temperature of the α-α' transition below the α-α'-β triple-point temperature, thus erasing the α-α' transition. While the model used here predicts the depression of the α-α' coexistence curve for 5% Mo, it is unable to predict the transition to the β phase. (This is because there is no mechanism built into the model for dealing with ordered phases. Although the CVM can in general be used to predict transitions to ordered phases, it is not a practical approach to take on this lattice because the clusters and configurations necessary to account for the β phase with random site energies become too numerous.) At 15% Mo the present calculations are comparable with the Monte Carlo result, the large depression of the critical point being due to the wide energy distribution (see Table II).

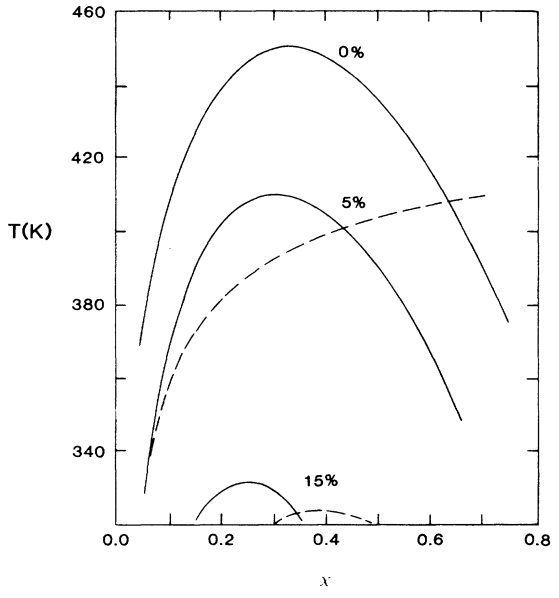

FIG. 4. Phase diagram for $Nb_{1-y}Mo_yH_x$ for 0%, 5%, and 15% Mo in Nb, as indicated. The solid curves are the results obtained in this work, and the dashed curves are the Monte Carlo results of Shirley *et al.* (Ref. 10) for the same model at 5% and 15%.

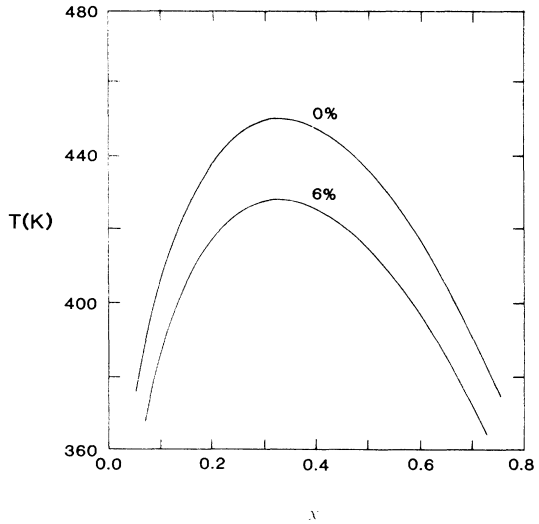

FIG. 5. Phase diagram for the α-α' transition in $Nb_{1-y}V_yH_x$ for 0%, and 6% V in Nb, as obtained in this work.

In contrast, the depression of the critical point is less severe in Nb-V-H enabling our model to provide a simple and yet more realistic description of the phase digram. As shown in Fig. 5, the model predicts a critical point for $Nb_{0.94}V_{0.06}H_x$ of $T_c = 428$ K, $x_c = 0.33$ (compared with 451 K, 0.33, respectively, for NbH_x), a decrease in critical temperature of 23 K in the alloy. The Monte Carlo calculations of Grewell give the critical temperature as 435 K for NbH_x and 418 K for the alloy, a decrease of 17 K. These results may be compared with the experimentally observed decrease of approximately 26 K from 444 to 418 K.[22,23]

It is informative to describe the effect on the phase diagram of varying some of the parameters of the model. Figure 6 shows the effect of increasingly better discrete approximations to a continuous random-energy distribution. The interaction energies are assumed to be those of Nb-H and the distribution $\rho(\epsilon)$ is taken to be rectangular with width $2000k_B$ K. The numbers on each curve correspond to the number Γ of equispaced energies being used to approximate the distribution, and range from $\Gamma = 1$ (no random energies) to $\Gamma = 13$. Fairly consistent results are achieved for $\Gamma \geq 5$, although this is a uniform, well-behaved, distribution and more complicated distributions can require larger values of Γ. However, the results do show that the discrete approximation can give good results for relatively small values of Γ.

The effect of increasing the separation ϵ_0 of the levels of a simple bilevel distribution is shown in Fig. 7. For the distribution, each lattice site must have energy 0 (with

TABLE II. Discrete random-energy distributions used in the calculation of the Nb-Mo-H and Nb-V-H phase diagrams.

Mo in Nb				V in Nb	
5%		15%		6%	
ϵ_α/k_B K	a_α	ϵ_α/k_B K	a_α	ϵ_α/k_B K	a_α
−300	0.020	−400	0.003	−650	0.0108
0	0.636	0	0.313	−480	0.0476
400	0.132	600	0.194	−340	0.1256
800	0.020	1600	0.260	−120	0.1948
1600	0.159	2200	0.113	0	0.4329
2100	0.020	3200	0.078	180	0.0606
3500	0.013	3800	0.021	320	0.1169
		4400	0.008	620	0.0108
		4900	0.010		

probability $\frac{1}{2}$) or energy ϵ_0 (with probability $\frac{1}{2}$); that is, $\rho(\epsilon)=\frac{1}{2}[\delta(0)+\delta(\epsilon_0)]$. Curves are drawn for $\epsilon_0/k_B=0$, 500, 1000, 1500, and 2000 K, with J_n again taken to be those of Nb-H. As the distribution widens the critical temperature initially decreases slowly, then shows a more rapid decrease which again slows as the separation becomes much greater than $1000k_B$ K. The critical concentration also shows a similar decrease. This dependence on the general width of the distribution is typical of all distributions considered.

Last, the effect of varying the range L of the H-H interactions is shown in Fig. 8 for Nb-H. Values of L are attached to each curve and some critical points are also shown. The critical temperature gradually increases as L increases, from a value of 277 K when there are no pair interactions, apart from the hard core, up to 451 K for $L=50$. For these calculations the long-range elastic term a depends upon L.[10,14–16] For $L\gtrsim 40$ there is only a small change in T_c, which shows that this is a sufficient number of shells to realistically describe the phase behavior.

Some final comments should also be made concerning the computation of the concentrations x_α. At small c the concentrations x_α are found to be proportional to $\exp(-\epsilon_\alpha/k_BT)$, as would be expected. This behavior is of assistance when selecting initial estimates of x_α to satisfy Eq. (34). For very wide distributions (such as $3000-4000k_B$ K), and as c increases, the minimized values of x_{α_0} for the lowest energy ϵ_{α_0} can tend linearly to $x_{\alpha_0}=0.2$. This concentration corresponds to all sites of

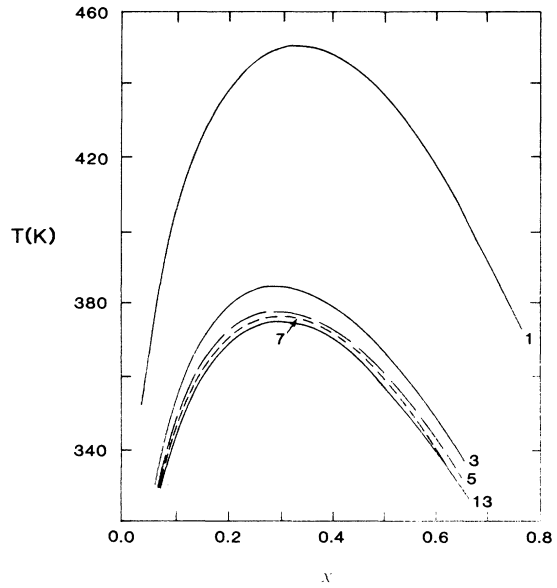

FIG. 6. Phase diagram for a model of increasingly finer discrete approximations to a continuous rectangular random-energy distribution. The number Γ of discrete energy levels is indicated for each curve.

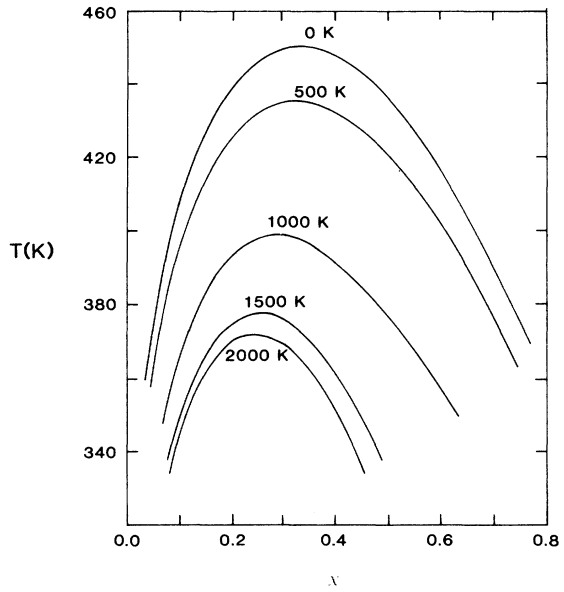

FIG. 7. Phase diagram for a random-energy distribution with two discrete energy levels of increasing separation ϵ_0. The value ϵ_0/k_B is attached to each curve.

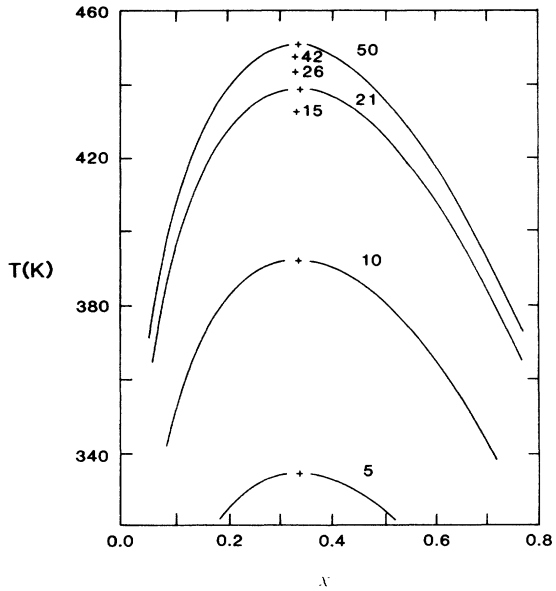

FIG. 8. The effect on the NbH_x phase diagram of variations in the maximum number L of nth-neighbor H-H interactions. A value of L is attached to each curve and some extra critical points (crosses) are also shown.

energy ϵ_{α_0} being occupied. In this case x_{α_0} is no longer a variable; the number of variables in Eq. (34) is decreased by one, with x_{α_0} set constant at 0.2. This effect seems to be an artefact of the approximations inherent in the model, but does not lead to any problems when solving the equation.

VI. CONCLUSION

The CVM has been applied to a random-field lattice system. Although the technique is quite general, the theory has been specifically applied to obtain a relatively simple expression describing the disorder-disorder phase transition in hydrogen-niobium alloy systems for small concentrations of the alloying element. The model requires the hydrogen interaction energies J_n and the random site energy distribution due to the effect of the alloying element; these parameters have been calculated for some alloys by other workers.

Good results are obtained for NbH_x and $Nb_{0.94}V_{0.06}H_x$. Since the model does not account for transitions to ordered phases the results for $Nb_{1-y}Mo_yH_x$ are not as good. Previous Monte Carlo calculations and experiments have shown that the α-α' transition is erased for Mo concentrations as small as 5%, leaving only the α-β transition. The model used here yields the large depression in critical temperature but because no allowance is made for the occurrence of the β phase a sensible comparison is not possible at higher molybdenum concentrations.

Although the CVM, in the model used here, is not capable of accounting for the ordered β phase some account of ordering can be made by using sublattices corresponding to the ground states that will occur. Work on such theory is in progress but at present has not been successful.

ACKNOWLEDGMENTS

The authors gratefully acknowledge the support of the National Science Foundation under Grant No. CHE-8514808.

[1]T. L. Hill, J. Chem. Phys. **17**, 762 (1949).
[2]T. Schneider and E. Pytte, Phys. Rev. B **15**, 1519 (1977).
[3]G. Grinstein and S. K. Ma, Phys. Rev. B **28**, 2588 (1983).
[4]T. Morita, J. Phys. Soc. Jpn. **14**, 563 (1959).
[5]T. Morita, Physica **119A**, 143 (1983).
[6]P. M. Richards, Phys. Rev. B **30**, 5183 (1984).
[7]J. M. Sanchez and D. de Fontaine, Phys. Rev. B **17**, 2926 (1978).
[8]J. A. Barker, Proc. R. Soc. London, Ser. A **216**, 45 (1953).
[9]C. K. Hall, A. I. Shirley, and P. S. Sahni, Phys. Rev. Lett. **53**, 1236 (1984).
[10]A. I. Shirley, C. K. Hall, P. S. Sahni, and N. J. P. King, J. Chem. Phys. **81**, 4053 (1984).
[11]P. C. Grewell, B. S. E. thesis, Princeton University, 1984. Grewell used the techniques and data sources of Refs. 14–16 to calculate the elastic H-metal and H-H interactions. The H-metal interactions were calculated from the pure-metal data assuming linear combination of the interactions. The random-site-energy distribution was calculated using the methods of Ref. 10. The long-range elastic interaction $a = -18\,412k_B$ K was obtained from Ref. 16, as in this work.
[12]P. M. Richards, Phys. Rev. B **28**, 300 (1984).
[13]G. Boureau, J. Phys. Chem. Solids **45**, 973 (1984).
[14]H. Wagner and H. Horner, Adv. Phys. **23**, 587 (1974).
[15]H. Horner and H. Wagner, J. Phys. C **7**, 3305 (1974).
[16]M. Futran, S. G. Coats, C. K. Hall, and D. O. Welch, J. Chem. Phys. **77**, 6223 (1982).
[17]D. de Fontaine and R. Kikuchi, National Bureau of Standards Publication No. SP-496 (1978) (unpublished).
[18]G. Boureau, J. Phys. Chem. Solids **42**, 743 (1981).
[19]P. Meuffels and W. Oates, J. Less-Common Met. (to be published).
[20]H. Zabel and J. Peisl, J. Phys. F **9**, 1461 (1979).
[21]U. Potzel, J. Völkl, H. Wipf, and A. Magerl, J. Less-Common Met. **103**, 182 (1984).
[22]M. A. Pick and D. O. Welch, Z. Phys. Chem. **114**, 37 (1979).
[23]J. Bethin, D. O. Welch, and M. A. Pick (unpublished).